Multi-wavelength fluorescence in image-guided surgery, clinical feasibility and future perspectives

Beurden, F. van; Willigen, D.M. van; Vojnovic, B.; Oosterom, M.N. van; Brouwer, O.R.; Poel, H.G. van der; … ; Buckle, T.

Review Article

Multi-Wavelength Fluorescence in Image-Guided Surgery, Clinical Feasibility and Future Perspectives

Florian van Beurden[1,2], Danny M. van Willigen[1], Borivoj Vojnovic[3], Matthias N. van Oosterom[1,2], Oscar R. Brouwer[1,2], Henk G. van der Poel[2], Hisataka Kobayashi[4] ⓘ, Fijs W.B. van Leeuwen[1,2,5], and Tessa Buckle[1,2] ⓘ

Abstract

With the rise of fluorescence-guided surgery, it has become evident that different types of fluorescence signals can provide value in the surgical setting. Hereby a different range of targets have been pursued in a great variety of surgical indications. One of the future challenges lies in combining complementary fluorescent readouts during one and the same surgical procedure, so-called multi-wavelength fluorescence guidance. In this review we summarize the current clinical state-of-the-art in multi-wavelength fluorescence guidance, basic technical concepts, possible future extensions of existing clinical indications and impact that the technology can bring to clinical care.

Introduction

The limited ability to visually discriminate surgical targets from surrounding tissues has driven the demand for image guidance technologies. The ability of fluorescence imaging to "illuminate" and provide real-time visualization of surgical targets in relation to their anatomical context has driven its increasing impact on surgical care.[1] Various fluorescent dyes have already been approved for clinical use (Table 1), namely Fluorescein, indocyanine green (ICG), 5-ALA/HAL-induced PpIX (PpIX[5-ALA] or PpIX[HAL]) and methylene blue (MB). These clinically approved fluorescent agents are broadly applied in a range of image-guided surgery indications, varying from lymphatic mapping to neurosurgery. In recent years an increasing number of new fluorescent tracers with different fluorescent signatures, either as a free dye or as dye conjugated to a targeting moiety, have found their way into first-in-human trials. Examples of alternative dyes (Table 1) that have been (or are being) implemented in clinical studies are: Cy5,[8] Cy7,[10] IRDye800CW,[12] SO456,[14] IRDye 700DX,[15] SGM-101[17] and ZW800-I.[19] Combined these fluorescent dyes/tracers yield a colorful palette of chemicals that can be used to stain a wide variety of diseased or anatomical structures.

The obvious starting point in fluorescence-guided surgery is the identification of individual features. However, visualization of a single feature during surgery does not provide a full answer to the anatomical complexity that surgeons encounter. Here combined use of complementary fluorescent tracers, also called multi-wavelength fluorescence imaging (or fluorescence multiplexing, multispectral fluorescence), could help to create an intraoperative atlas of the most important pathologies and physiological parameters.[20] The feasibility of this concept is underlined by the fact that it is already routinely applied in diagnostic ophthalmology,[21] where the fluorescent dyes Fluorescein and

[1] Interventional Molecular Imaging Laboratory, Department of Radiology, Leiden University Medical Center, Leiden, The Netherlands
[2] Department of Urology, The Netherlands Cancer Institute-Antoni van Leeuwenhoek Hospital, Amsterdam, The Netherlands
[3] Department of Oncology, Cancer Research UK/MRC Oxford Institute for Radiation Oncology, University of Oxford, Oxford, United Kingdom
[4] Molecular Imaging Program, Center for Cancer Research, National Cancer Institute, National Institutes of Health, Bethesda, MD, USA
[5] Orsi Academy, Melle, Belgium

Corresponding Author:
Tessa Buckle, Interventional Molecular Imaging Laboratory, Department of Radiology, Leiden University Medical Center, Albinusdreef 2 (C2-S zone), PO BOX 9600, 2300 RC Leiden, The Netherlands.
Email: t.buckle@lumc.nl

Table 1. Fluorescent Dyes Used in Clinical Applications.

			Clinically approved dyes		
Compound	Excitation (nm)	Emission (nm)	Quantum yield (%)	Molar absorption coefficient (L*Mol^{-1}*cm^{-1})	Brightness
Fluorescein[2,3]	488 (PBS)	515 (PBS)	12 (HSA)	40000 (HSA)	4800
ICG[4]	807 (FBS/HEPES)	822 (FBS/HEPES)	9,3 (FBS/HEPES)	121000 (FBS/HEPES)	11253
Methylene blue[4]	665 (FBS/HEPES)	688 (FBS/HEPES)	9,6 (FBS/HEPES)	49500 (FBS/HEPES)	4752
PpIX[5-ALA/HAL 5-7]	404 (PBS)	634	4,1 (HSA)	4866	200
			Dyes applied in clinical studies		
Compound	Excitation (nm)	Emission (nm)	Quantum yield (%)	Molar absorption coefficient (L*Mol^{-1}*cm^{-1})	Brightness
Cy5[8,9]	650 (PBS)	667 (PBS)	27 (PBS)	250000 (PBS)	67500
Cy7[9-11]	750 (PBS)	777 (PBS)	2,6 (PBS)	200000 (PBS)	5200
IRDye800CW[12,13]	774	788	14,2 (FBS/HEPES)	237000	33654
SO456[14,13]	776	793	15,1	272000	41072
IRDye 700DX[15,16]	689	700	14	170000	23800
SGM-101 (BM-104)[17,18]	685 (pH 6 buffer)	705 (pH 6 buffer)	17 (Buffer)	N.R.	N.A.
ZW800-1[19,13]	772	788	15,1 (FBS/HEPES)	249000	37599

NR=not reported, N.A. = not available, could not be calculated.

ICG are simultaneously used to respectively visualize the retinal and choroidal vasculature.

When considering that the use of complementary fluorescent dyes during surgery can support visualization of separate surgical targets (for instance: vasculature, lymph nodes/drainage, malignant tissue or even nerves), multi-wavelength fluorescence imaging could also allow differentiation between surgical targets and surrounding vital structures or to detect different molecular targets within a single lesion. This concept could further enable e.g. oncological surgeons to strive toward radical resections with minimal procedural side-effects and would thereby pave the way for precision surgery (precision surgery can be defined as disease (or tissue) specific resections) as realized by image-guided surgery concepts such as multi-wavelength fluorescence surgery. For multi-wavelength fluorescence imaging to be routinely used in the clinic, availability of fluorescent dyes/tracers that emit signal at different wavelengths obviously needs to go hand in hand with innovations in imaging technologies that support the detection of different fluorescent emissions.

This review aims to deliver a comprehensive overview of the clinical studies that have addressed the implementation of multi-wavelength fluorescence imaging in humans. Besides the real-time visualization of different fluorescent emissions, the more commonly used sequential fluorescence imaging approaches are also mentioned. In order to provide a translational focus, only pre-clinical efforts that overlap with applications already explored in the clinic were included. Thereby the current manuscript does not attempt to provide a comprehensive overview of all pre-clinical multi-wavelength endeavors, but rather focusses on the translational aspects. In relation to the clinical implementation and in relation to pre-clinical efforts, future perspectives based on new chemical- and engineering-innovations are briefly discussed.

Technical Aspects Behind Multi-Wavelength Fluorescence Imaging

Obviously, the distribution of a fluorescent agent in human body plays an essential role in the visualization of targeted tissues. Where some agents have been designed for angiographic purposes (Fluorescein and ICG), or lymphatic drainage (MB), others have been designed to provide a measure for metabolism (5-ALA and HAL). Besides many different dyes, currently, even nanoparticles and receptor targeted fluorescent agents are finding their way into clinical applications. All these applications, however, demand a substantially different molecular composition of the imaging agent. As certain applications even demand tailoring of the biological clearance pathway and background accumulation,[22] we feel it is difficult, if not impossible, to provide generic guidelines in tracer design. We have, therefore, not made an attempt to address this issue, but have focused our technical overview on the photophysical aspects

that drive the successful implementation of multi-wavelength fluorescence imaging.

To fully understand how multi-wavelength fluorescence imaging can be applied in an image-guided surgery setting, a basic level of understanding of the underlying technical and photophysical aspects is required. Key technical aspects relevant for the camera systems used for multispectral fluorescence imaging, are the spectral overlap (ability to separate fluorescence signals), the brightness of dyes (signal intensity) and wavelength dependent light-tissue interactions of dyes (signal intensity and background in the form of autofluorescence and scattering).

Spectral Separation of Signals

A key element in multi-wavelength fluorescence imaging is the ability to separately detect light that is emitted by different dyes at different wavelengths during excitation by similar or separate wavelengths. Other than nuclear medicine-based multiplexing solutions such as dual-isotope SPECT,[23] wherein detection of multiple signals takes place based on spontaneous emitted energies, in fluorescence imaging an excitation-light source needs to be tuned to the specific characteristics of a fluorescent dye. A signature characteristic of a fluorescent dye is its light-absorbance and -emission profile. The differences between these profiles (Table 1) indicate that each dye has an optimal excitation and emission window. As these profiles are not entirely distinct, spectral profiles can partially overlap. In these cases, differences in Stokes-shift (spectral spacing between $\lambda_{ex\ max}$ and $\lambda_{em\ max}$) might enable differentiation between different dyes.

Since surgery is still predominantly performed under white-light imaging, this means that, next to allowing white-light imaging, multi-wavelength fluorescence cameras have to include both wavelength-specific excitation sources and wavelength-specific imaging detectors.

For excitation either different wavelength specific light sources such as lasers or LEDs, filtering of a light source with a broad spectrum (e.g. xenon or halogen lamp) or combinations of these approaches can be used.[24] Hereby signal intensities impact on the photon flux of the dyes embedded within the tissue. When different fluorescent dyes are used, excitation at different wavelengths allows excitation of spectrally separate fluorescent dyes.[25] Assuming that the detector used is sensitive over the desired spectral range, the emitted fluorescence signals can be separately detected through spectral separation, e.g. by applying bandpass, notch, or dichromatic mirrors in front of the detector.[24,26] Alternatively, either full or partial spectral separation can occur via image processing. Despite using wavelength specific detectors, cameras may detect "false" readings as related to ambient light, a feature that is particularly challenging in an open surgery setting.[1]

Signal collection can be realized using 2 different approaches; either through sequential imaging using different excitation sources and emission filters tailored for each dye specifically, or by applying simultaneous excitation and detection of the respective dyes. For sequential imaging of complementary dyes that exhibit minimal spectral overlap (e.g. Fluorescein, ICG and Cy5), clinically approved fluorescence laparoscope set-ups can be used if they are fitted with a switchable filter wheel for excitation and emission (Karl STORZ Endoskope GmbH).[3] In this approach sequential imaging limits the chance of spectral overlap of the different emission signals. Sequential imaging does, however, not allow simultaneous visualization of complementary features in real-time.

Simultaneous imaging of dyes becomes possible when excitation can occur at multiple wavelengths. For instance, in fluorescence imaging mode, the Firefly laparoscope (Intuitive Surgical Inc.) employs an excitation laser for ICG with a band of complementary blue LED light that can be used to excite Fluorescein.[27] In this system all light is detected by a single full-color camera, allowing visual separation of, in this case, Fluorescein and ICG (note: this only applies when no or specific image processing is applied). This real-time imaging approach allows concurrent differentiation of structures, e.g. prostate and neurovascular bundle, without switching between excitation and emission filters during the procedure.[27] Alternatively, simultaneous multi-wavelength fluorescence imaging set-ups that include multiple (filtered) detectors (i.e. an imaging detector for each individual signal) can be used, after which the video output from the different detectors is merged.[28] Following image acquisition, different processing solutions are available that can be used to resolve the spectral contribution of each separate fluorescent tracer, such as linear unmixing, principal component analysis and supervised classification.[29,30]

Signal Intensities of Dyes

As with any other form of molecular imaging, signal intensities are instrumental for the use of fluorescence during image-guided surgery applications. In essence, the fluorescence intensities in surgically interesting anatomies have to be high enough to allow for their separation from surrounding tissue (so-called signal-to-background ratio).[31,32] Clearly, here the biological behavior of a fluorescent imaging agent is of upmost importance. If the fluorescent agent does not accumulate in a specific cell type, tissue type, or anatomy, it simply cannot be used for imaging. Assuming only effective fluorescent agents are considered for clinical translation, maximal dye excitation and a high emission detection efficacy remain critical. The first requires spectral overlap of the excitation light source with the $\lambda_{ex\ max}$ of a particular fluorescent dye, while for the second requirement, emission filtering complementary to the $\lambda_{em\ max}$ needs to be applied. However, next to spectral variations between fluorescent dyes, the intensity of a fluorescent emission is also substantially influenced by photophysical properties such as absorption coefficient (ability of a dye to absorb excitation light) and quantum yield (ability of a dye to convert the absorbed energy into a fluorescent emission) of individual dyes.

Together with the excitation light intensity and dye concentration these photophysical factors determine the fluorescence brightness (Table 1).[33] As the human eye functions with a pretty high sensitivity and allows separation in the visible range of light, fluorescent dyes that emit in the visible light spectrum can even be differentiated by the naked eye.[34,35]

Light-Tissue Interactions

One should realize that both the excitation light coming from the camera and the light emitted by the dye embedded in the anatomy interact with tissue. In literature much has been said about the ability of different fluorescence emissions to penetrate through (human) tissues.[36] In particular light absorbance and light scattering of e.g. endogenous molecules are key tissue properties that impair the penetration of fluorescent emissions through tissue.[36,37] Overall, assuming an identical light intensity, external excitation light and internal fluorescent emissions show superior tissue penetration at higher wavelengths. This argument has been extensively used to promote the use of near-infrared (NIR) fluorescence (λ_{em} 700-950 nm; e.g. ICG) in the field of image-guided surgery.[38] Nevertheless, current surgical literature indicates that even NIR fluorescence imaging is impaired in its effective working distance; fluorescent lesions can provide intraoperative guidance when located < 10 mm from the surface.[39] More recently researchers have explored the NIR II spectrum (1000-1700 nm), a spectral region wherein scattering and autofluorescence are said to be reduced even further, thereby claiming these wavelengths enhance the tissue penetration and signal resolution.[40]

Excitation light sources may elicit fluorescent emissions from endogenous compounds, yielding so-called autofluorescence. Endogenous dyes (e.g. flavins, flavoproteins, collagen, and elastin, NADH and other redox controllers) may yield background signals that can impact the signal-to-background ratio, impairing the detection of dye-related fluorescence within that tissue. Most endogenous dyes are excited at lower wavelengths (400-450 nm) and emit in the 510 to 550 nm range[41,42] while their broad emission spectrum can be observed even in the NIR range, given appropriate imaging sensitivity. Despite the low fluorescence brightness, autofluorescence of endogenous dyes can be used to provide tissue specific surgical-guidance during e.g. parathyroid surgery.[43,44]

Combination of these technical and photophysical traits indicates that the photophysics of dyes, imaging hardware and the composition of tissue all have the potential to impact the surgical implementation of multi-wavelength fluorescence imaging strategies, making it a technically challenging endeavor. Moreover, the tradeoffs between technical (e.g. resolution, field of view) and physiological traits (e.g. background fluorescence) can also slightly differ per indication. That said, the fact that fluorescence guidance during surgery is predominantly used as a technique to detect lesions/anatomies at or very near to the tissue surface, simplifies some aspects.

Indications

Neurosurgery

Multiplexing Fluorescein and ICG. Both the fluorescent dyes Fluorescein and ICG have been applied for angiographic purposes and intracranial glioma imaging; the pathological growth of vasculature in gliomas disrupts the blood brain barrier, causing both Fluorescein and ICG to extravasate into the extracellular space.[45,46] The routine clinical use of Fluorescein and ICG in neurosurgery and the availability of matching clinical grade cameras, surgical microscopes and endoscopes provided an ideal platform for the technical exploration of multi-wavelength fluorescence imaging approaches (Table 2).

Acerbi et al. exploited the differences in emission profiles of Fluorescein and ICG (Table 1) to separate high-grade glioma tumors form their surrounding vasculature using videoangiography.[47] Fluorescein was administered directly after intubation, where after it was allowed to leak in the extracellular space of the lesion. ICG administration was conducted intraoperatively and was used to visualize the vascular structures. Lane et al.[48] exploited the short arterial phase of both dyes to sequentially perform angiography during aneurysm clipping (Figure 1A). After clip placement ICG was used to assess exclusion of the aneurysm. Lack of exclusion required repositioning of the clip, with a subsequent angiographic reassessment using Fluorescein to prevent overlap with background signals from the previously administered ICG.[48] Despite the proven technical feasibility to use both Fluorescein and ICG for angiographic purposes, one should consider that ICG videoangiography is the current clinical standard and also the authors of the multi-wavelength studies indicate it is to be preferred over Fluorescein videoangiography.[48,65]

Multiplexing Fluorescein and PpIx^{5-ALA}. 5-ALA is commonly used to identify high grade gliomas via their ability to metabolically convert 5-ALA into the fluorophore protoporphyrin IX (PpIX^{5-ALA})[46] and has recently been FDA-approved for glioblastoma surgery. During fluorescence-guided surgery $PpIx^{5-ALA}$ based contrast-enhancement has been shown to enable more complete tumor resections, and progression-free survival in patients with malignant glioma.[66] Despite being used for similar indications, both $PpIx^{5-ALA}$ and Fluorescein have inherently different tumor staining characteristics; like ICG (see above), Fluorescein accumulates in the extracellular space in tumor areas with a disrupted blood-brain barrier (BBB), while PpIX^{5-ALA} signal is highest in tissues with a high metabolic rate.[49,67]

Della Puppa et al.,[50] Yano et al.[51] and Schwake et al.[52] all reported that in a multi-wavelength procedure Fluorescein could be used to demarcate extravasation into the necrotic bulk of a (high-grade) brain tumor, while the fluorescence signal of PpIX^{5-ALA} helped to define the viable tumor margins.[50-52] In a study in patients harboring suspected malignant glioma Suero Molina et al. described that besides facilitating the surgeon to assess tumor heterogeneity, addition of Fluorescein supported the discrimination of healthy brain parenchyma, and in doing

Table 2. Clinical Applications Multi-Wavelength Fluorescence Imaging.

Author	Indication	N =	Dyes used	Type of imaging set-up	Camera system
Neurosurgery					
Acerbi et al, 2016[47]	Differentiation between high-grade glioma and surrounding vasculature	3	Fluorescein ICG	Simultaneous	YELLOW 560 microscope system; Carl Zeiss (FDA approved) FLOW 800 microscope system; Carl Zeiss (FDA approved)
Lane et al, 2015[48]	Sequential angiographic imaging of complex cerebral aneurysms	22	Fluorescein ICG	Sequential	YELLOW 560 microscope system; Carl Zeiss (FDA approved) FLOW 800 microscope system; Carl Zeiss (FDA approved)
Francaviglia et al, 2017[49]	Evaluation complete resection of high-grade gliomas	47	Fluorescein PpIX[5-ALA]	Simultaneous	OPMI Pentero 900 microscope + Yellow 560 filter (Carl Zeiss)
Della Puppa et al, 2019[50]	Staining different molecular properties of glioblastoma to enhance sensitivity	3	Fluorescein PpIX[5-ALA]	Simultaneous	Yellow 560 microscope system; Carl Zeiss (FDA approved) Blue 400 microscope system; Carl Zeiss (FDA approved)
Yano et al, 2017[51]	Staining different molecular properties of glioblastoma to enhance sensitivity	8	Fluorescein PpIX[5-ALA]	Simultaneous	Laparoscopic D-light system; Storz (FDA approved)
Schwake et al, 2015[52]	Staining different molecular properties of glioblastoma to enhance sensitivity	4	Fluorescein PpIX[5-ALA]	Simultaneous	FL560 (M530 OH6; microscope); Leica (FDA approved) equipped with a FL400 filter; Leica microscope (FDA approved)
Suero Molina et al, 2019[53]	Differentiation between high-grade glioma and surrounding tissue	6	Fluorescein PpIX[5-ALA]	Simultaneous	modified experimental xenon light system (ex 390–475 nm; Carl Zeiss Meditec. CE marked), integrated into a standard OPMI Pentero microscope + BLUE 400 filter
Suero Molina, 2018[54]	Staining different molecular properties of brain stem malignancies to enhance sensitivity	1	Fluorescein PpIX[5-ALA]	Simultaneous	Yellow 560 system; Zeiss microscope (FDA approved) Blue 400 system; Zeiss (FDA approved)
Eyüpoglu et al, 2015[55]	Staining different molecular properties of glioblastoma to enhance sensitivity	3	ICG PpIX[5-ALA]	Simultaneous	OPMI Pentero; Zeiss microscope (FDA approved) No further specifics are reported
Bladder cancer					
Marien et al, 2017[56]	Diagnosis assisted trans urethral dissection bladder cancer	21 (ex vivo)	Fluorescein PpIX[HAL]	Simultaneous	GastroFlex; Cellvizio fiber-confocal microscope (FDA approved) Ultra Mini O Probe; Cellvizio fiber-confocal microscope (not-FDA approved) Exera II endoscopic system; Olympus (FDA approved)
Kriegmair et al, 2020[57]	Real-time diagnosis of malignant bladder lesions	10	PpIX[HEXVIX] Autofluorescence	Simultaneous	Custom built camera system equipped with PDD endoscopes (Karl STORZ WL, enhanced vascular contrast (EVC), blue light fluorescence, protoporphyrin IX fluorescence, and autofluorescence.
Hepatic lesions					
Kaibori et al, 2016[58]	Ddetection of surface related liver tumors	48	ICG PpIX[5-ala]	Sequential	-Photodynamic eye wide field fluorescence camera (PDE); Hamamatsu photonics (FDA approved) + specific blue light (prototype); SBI pharmaceuticals +additional filter
Hu et al, 2019[40]	Detection of surface related liver tumors	23	ICG NIR I ICG NIR II	Simultaneous	Custom built prototype; PCO.edge 5.5 m; PCO AG) enabling NIRvana 640; Teledyne Princeton Instruments

Table 2. (continued)

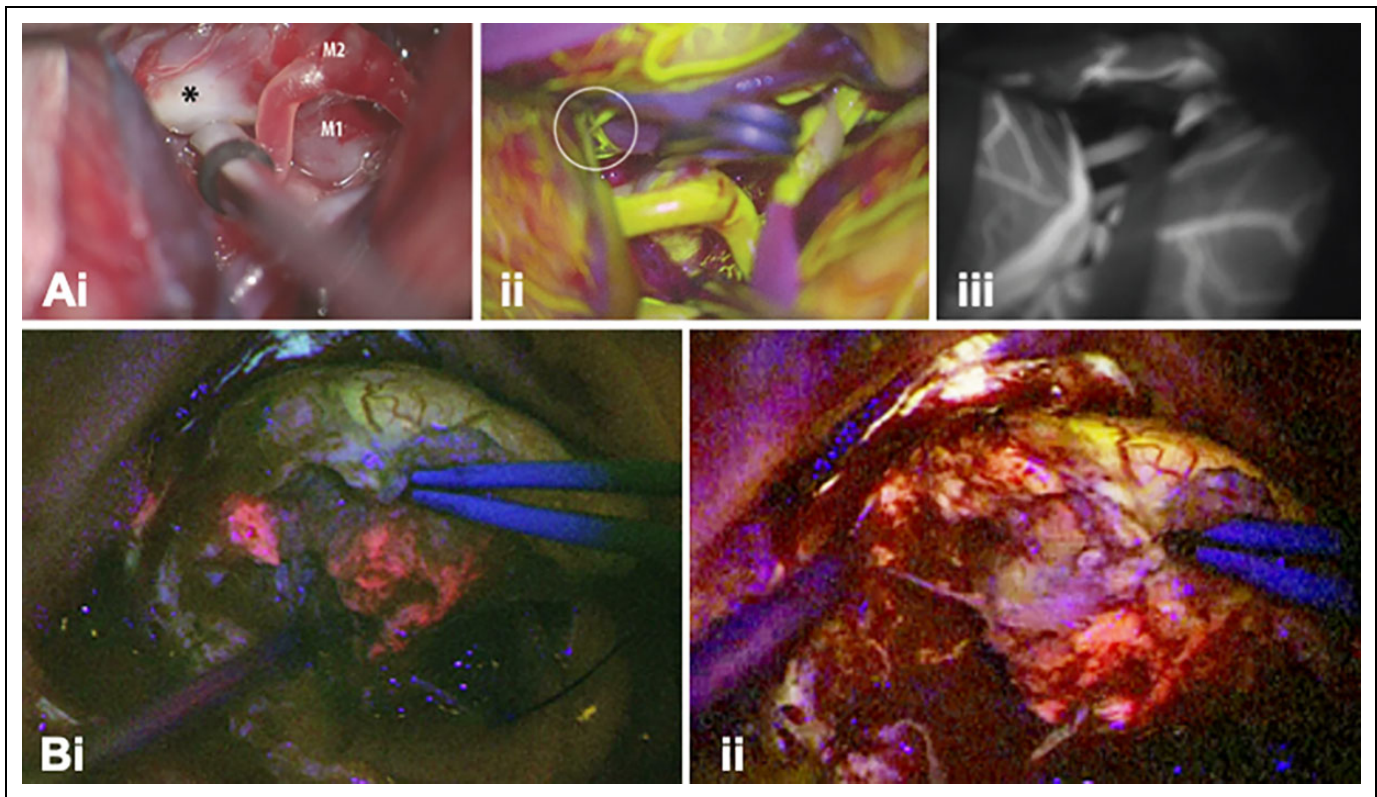| Author	Indication	N =	Dyes used	Type of imaging set-up	Camera system
Parathyroid					
Kahramangil et al, 2017[59]	Identification parathyroid glands	22	ICG Autofluorescence Parathyroid	Sequential	Not specified
Alesina et al, 2018[60]	Identifying parathyroid glands and their vascularization during thyroidectomy	5	ICG Autofluorescence Parathyroid	Sequential & Simultaneous	IMAGE1S; Karl Storz endoscope (FDA approved)
Lerchenberger et al, 2019[61]	Identifying parathyroid glands and their vascularization during thyroidectomy	50	ICG Autofluorescence Parathyroid	Sequential	Image1 H3-Z 3-Chip Full HD camera; Karl Storz laparoscope (FDA approved)
Ladurner et al, 2019[62]	Identifying parathyroid glands and their vascularization during thyroidectomy	117	ICG Autofluorescence Parathyroid	Sequential	Image1 H3-Z 3-Chip Full HD camera; Karl Storz laparoscope (FDA approved)
Lymphatics					
Laios et al, 2015[63]	Determine association between injection site and SN detection using 2 different dyes	2	Methylene blue ICG	Simultaneous	Super HAD CCD II; Sony Hopkins II rigid laparoscope (prototype)
van den Berg et al, 2017[20]	Visualization of SN and the associated lymph ducts	10	Fluorescein ICG	Sequential	Image 1 HUB HD + D-light P system; Karl Storz laparoscope (FDA approved)
Plastic surgery					
Phillips et al, 2012[64]	Tissue perfusion during flap reconstruction	32	Fluorescein ICG	Sequential	SPY 2001 widefield Imaging System (Novadaq) Wood's lamp.

6

Figure 1. Multi-wavelength imaging in neurosurgery. (A-i) White light image of the surgical field through a microscope showing a left MCA bifurcation aneurysm (asterisk) with corresponding (ii) Fluorescein-based vascular angiography (FL-VA), and (iii) ICG-based vascular angiography (ICG-VA) (Adapted form Lane et al[48]). Intraoperative visualization of a left-frontal distant recurrence of a gliosarcoma via large field imaging with (B-i) a BLUE 400 filter (PpIX ^{ALA} in pink) and (ii) a YB 475 filter (Fluorescein in yellow) (Adapted from Suero Molina et al.[54]).

so, strengthened the contrast of the PpIX$^{5\text{-}ALA}$ signal. The mechanism behind staining of the healthy parenchyma is not in line with the intended use of the dye for extravasation in areas with a disrupted BBB. Nevertheless, this staining is said to allow the surgeon to perform surgery in real-time fluorescence mode (Figure 1B), without having to switch between illumination sources during the manipulation of tissue.[53] Implementation of this concept was later also attempted during the resection of brainstem malignancies but was unsuccessful due to insufficient accumulation of PpIX in the target lesion.[54]

Multiplexing PpIX$^{5\text{-}ALA}$ and ICG. The third dye combination that has been explored in neurosurgery is PpIX$^{5\text{-}ALA}$ and ICG. Eyüpoglu et al.[55] used sequential fluorescence imaging to remove the tumor bulk based on the PpIX$^{5\text{-}ALA}$ signal, after which administration of ICG allowed visualization of hypervascularization in the transitional zone. The authors indicate this approach enabled detection of hypervascularized glioma segments where the cell density was insufficient to provide a clear PpIX$^{5\text{-}ALA}$ signal. Postoperative immunostaining confirmed the resected hypervascularized areas to be invaded by glioma cells.[55]

Experimental extensions. In the preclinical setting the use of multi-wavelength fluorescence imaging based on PpIX and

ICG was used to spare ICG-stained vascular structures.[26] Unfortunately, the short biological half-life of ICG left only a short window of detection.[48]

A comprehensive review by Sender et al.[68] indicated different targeted probes conjugated to respectively Cy3 ($\lambda_{ex\ max}$: 550 nm, $\lambda_{em\ max}$: 565 nm), Cy5, Cy5.5 ($\lambda_{ex\ max}$: 675 nm, $\lambda_{em\ max}$: 694 nm), IRDye800CW and Alexafluor 488 ($\lambda_{ex\ max}$: 499 nm, $\lambda_{em\ max}$: 520 nm) were being evaluated for their use in preclinical neurosurgical approaches. With more of these dyes becoming available for in-human use in the near future, the amount of clinical applications that could benefit from multi-wavelength fluorescence imaging could expand even further.

Bladder Cancer

Fluorescein and PpIX^{HAL}. In surgical treatment of superficially located urothelial cell carcinoma, fluorescence guidance using PpIX^{HAL} (obtained after conversion of the metabolic marker HAL into PpIX) has been used to support tumor delineation.[69,70] A meta-analysis that compared the results of 6 clinical trials revealed that this improved detection led to a reduction of recurrence at 9-12 months from 45.4% to 34.5%.[70] Yet another study indicated HAL helps reduce recurrence rates from 30.9% to 13.6% during transurethral resection of the bladder (TURB).[71] A downside of PpIX^{HAL} mono-fluorescence
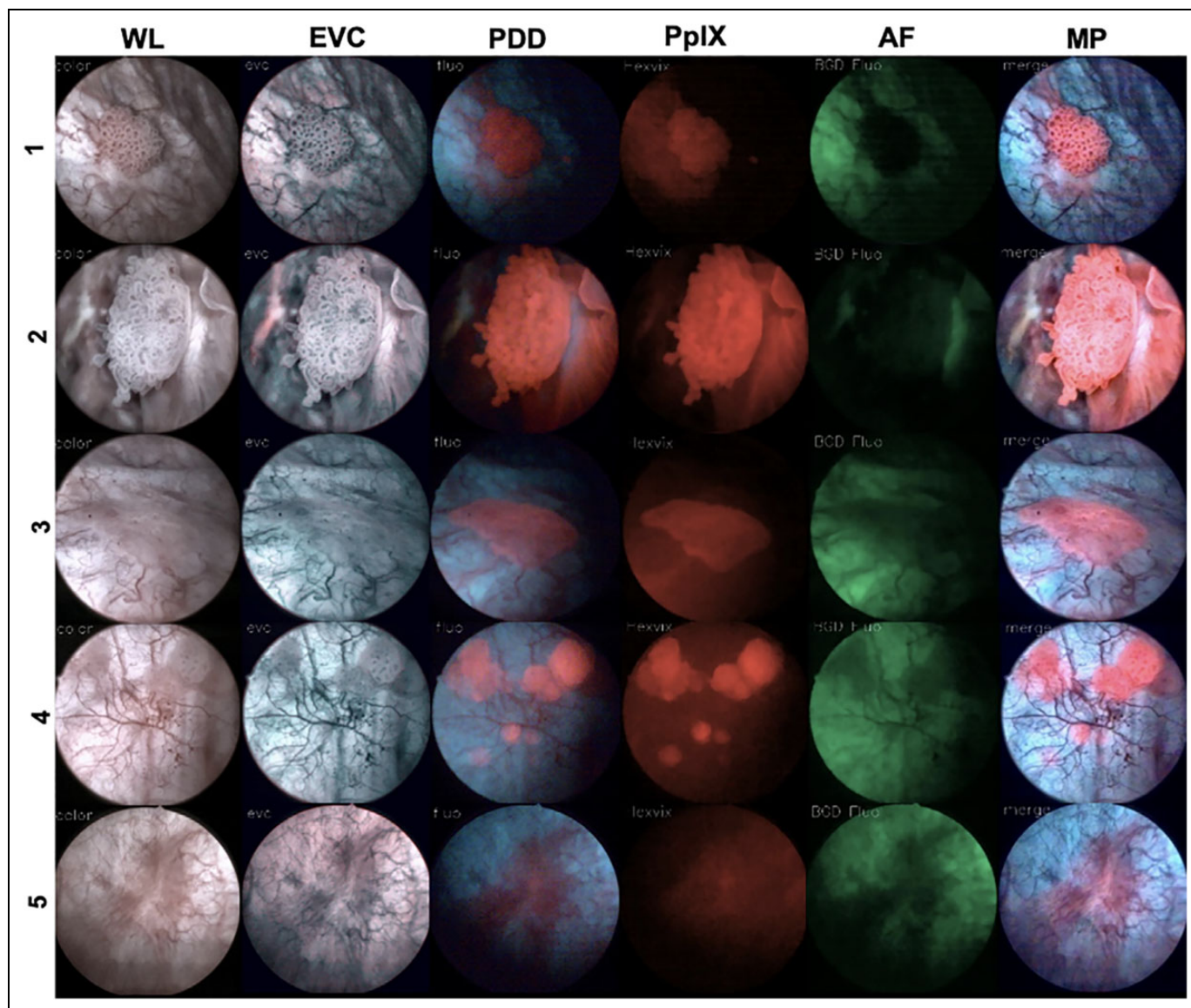
Figure 2. Multiparameter fluorescence imaging of bladder cancer. Representative cytoscopic imaging in 5 patients showing white-light (WL) images and enhanced vascular contrast (EVC), PDD, protoporphyrin IX fluorescence (PpIX-F), and autofluorescence (AF) characteristics. An overlay of all detected features is provided as a multiparametric image (MP) in real-time (adapted from Kriegmair et al.[57]).

imaging is the high percentage (65.5%) of false positives that occur due to the staining of high metabolic inflammatory tissue present in the bladder.[72] Alternatively, it has been shown that administration of Fluorescein into the urinary tract can be used to stain the extracellular matrix of urothelial cell carcinoma, thus providing information about the extracellular tumor structure and morphology when assessing the tissue using a fiber confocal-fluorescence microscope.[73]

Combined use of PpIX[HAL] and Fluorescein (Table 2) was applied during TURB, where it helped enhance both sensitivity and specificity.[56] *Ex vivo* multi-wavelength fiber confocal-fluorescence microscopic imaging of these 2 fluorescence signals provided information about cell contours (Fluorescein) and cell content (PpIX[HAl]), and with that, the

nucleocytoplasmic ratio. This provided a measure that is strongly suggestive for malignancy of bladder lesions and could aid the discrimination between cancerous and inflammatory tissue at a microscopic scale. Unfortunately, *in vivo* application of this approach during TURB has not yet been reported, nor are there indications the concept can be used for large field assessment of the bladder wall.

Autofluorescence and PpIX[HAL]. Recently, Kriegmair et al. used a multiparametric cystoscopy set-up (Figure 2, Table 2) wherein 5 modalities (intraoperative white light, enhanced vascular contrast, blue light fluorescence, protoporphyrin IX fluorescence (PpIX[HAL]) and autofluorescence of bladder tissue) were simultaneously applied to improve the detection of bladder cancer.[57]
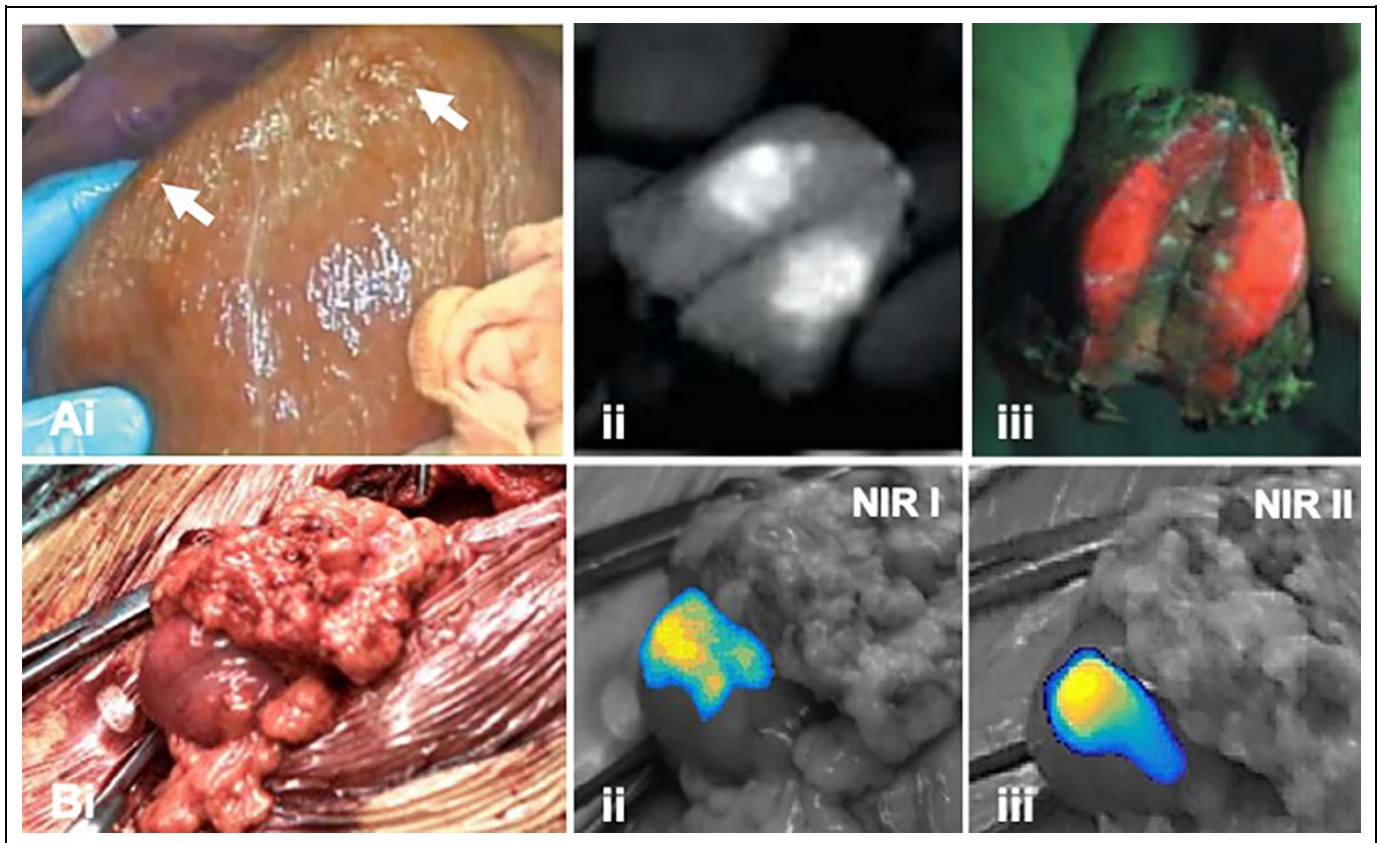
Figure 3. Multi-wavelength imaging of hepatic lesions. A, (i) Widefield imaging of the surgical field (liver) in white light indicating liver metastases (white arrow). Fluorescence images of incised lesion after illumination of (ii) ICG and (iii) PpIX[5ALA] (adapted from Kaibori et al[58]). B, (i) Widefield imaging in white-light image of a metastasis located in the omentum with corresponding (ii) NIR I and (iii) NIR II fluorescence images (adapted from Hu et al[40]).

In this approach enhanced vascular contrast and photodynamic images were merged into one real-time multiparametric image. Overall this study showed that real-time multiparametric assessment allowed identification of a higher number of malignant lesions compared to the individual modalities.[57]

Experimental extensions. Characteristics of tumor cells (or their surrounding tissues), such as receptor over-expression, can be used to specifically highlight malignant lesions. Therefore, the next step toward molecular endoscopy could be allowed by implementing of receptor-specific, fluorescently labeled tracers. Initial *ex vivo* evaluation of such fluorescent targeted tracers, in this case a CD47-targeting antibody conjugated with a Qdot (λ_{ex} = 405 nm, λ_{em} = 625 nm), has shown a sensitivity and specificity of 82.9% and 90.5% for CD47-based detection of malignancy in human cystectomy samples obtained from patients who underwent radical cystectomy for muscle invasive or high-risk non-muscle invasive bladder cancer.[74] Others have reported the use of anti-CD47 mAbs conjugated with Fluorescein or IRDye700DX in respectively *ex vivo* human cystectomy samples and, human bladder cancer cell lines and primary human bladder cancer cells derived from fresh surgical samples.[74,75]

Hepatic Lesions

PpIX[5-ALA] and ICG. In hepatocellular carcinoma (HCC) and hepatic colorectal metastasis the biliary ducts are often compressed by the tumor, causing impaired biliary excretion of ICG and hepatic clearance. This feature allows tumor delineation based on the presence of a fluorescent rim around the lesion that will remain visible for up to 2 weeks after intravenous administration,[76] an approach that has been explore in both open and laparoscopic surgery. PpIX[5-ALA] has been shown to effectively detect hepatocellular carcinoma cases with serosa invasion (100% of cases) and liver metastasis from colorectal cancer cases with serosa invasion (87.7% of cases), with a 92.5% sensitivity.[77] Moreover, Inoue et al. showed that malignant liver tumors could be completely removed based on PpIX[5-ALA] fluorescence resulting in significant smaller resection margins compared to white-light observation.[77]

In an open surgery setting, Kaibori et al.[58] demonstrated that sequential multi-wavelength fluorescence imaging of ICG and PpIX[5-ALA] supported the visualization of superficial hepatic lesions and peritoneal metastasis (Figure 3A, Table 2); intracellular staining reveals tumor metabolism (PpIX[5-ALA]) while physiological stasis of ICG contributes to a fluorescence signal in the extracellular space. Overall, ICG-guided detection
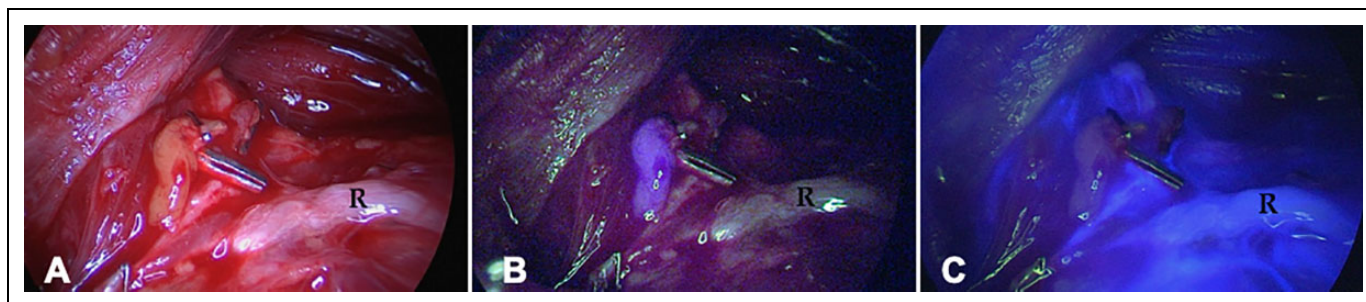
Figure 4. Parathyroid autofluorescence and ICG imaging. (A) Widefield white-light image of parathyroid glands (R = recurrent laryngeal nerve). (B) NIR-based autofluorescence signal of the parathyroid gland in blue and (C) NIR ICG fluorescence imaging showing the lack of vascularization of the parathyroid gland (ICG in blue; adapted from Ladurner et al.[62]).

proved to have a much higher sensitivity (94%) compared to PpIX[5-ALA]-based detection.[58]

ICG NIR I and NIR II. Besides emission in the NIR I region (700-950 nm) ICG also emits fluorescence in the NIR II window (1000-1700 nm). It has been suggested that fluorescence detection in the NIR II window may provide advantages over NIR I imaging, including improved imaging depth sensitivity, higher spatial resolution and imaging contrast. To this end, Hu et al. recently explored the utility of ICG emission in both the NIR I and NIR II spectral window in patients with hepatic lesions (open surgery setting; Figure 3B, Table 2).[40] Direct comparison between the 2 emissions suggested that the higher tumor-to-background ratios and higher tumor detection sensitivity that were obtained using NIR II imaging resulted in a higher positive predictive value compared to NIR I-based imaging of ICG.

Experimental extensions. In the preclinical setting several approaches are described that might also have value. For instance, the concomitant use of ICG and Fluorescein was shown to allow enhanced discrimination between healthy parenchyma and colorectal liver metastasis in murine models.[78] This approach could prove to be a useful asset in the quest to lower false positive rates of ICG-based fluorescence imaging of liver lesions (now 40%[79]). An alternative concept is the simultaneous visualization of both bile ducts and hepatic arteries using different combinations of ICG, MB and ZW800-I, as was assessed by Ashitate et al. in a porcine model.[80] NIR I and NIR II detection could further extend these efforts. Unfortunately, there are, to date, no FDA-approved dyes that are specifically designed for NIR II imaging.[81] Although somewhat more experimental, new dye-functionalized targeting agents, like SGM-101 (an antibody targeted to the carcinoembryonic antigen (CEA) conjugated to the fluorescent dye BM-104) have also shown potential in multiplexing applications for treatment of hepatic cancer; combined use of SGM-101 and ICG was shown to aid tumor detection (SGM-101) as well as identification of intrahepatic bile ducts and/or vasculature (ICG) in the reconstructive part of hepatic surgery.[82]

Parathyroid

Autofluorescence and ICG. Sparing of the parathyroid glands during thyroidectomy surgery can be challenging, as these glands and their feeding vascularization are hard to visually discriminate from the surrounding tissue. Intraoperative identification of the parathyroid glands has been evaluated extensively using autofluorescence (e.g. via the properties of the calcium-sensing receptor protein; CSRP).[83-86] Hereby, ICG angiography can be used to pre- and/or post-operatively assess the vascularization of individual glands and thus helps identify the gland as well as assess its viability and suitability for auto transplantation. In these studies, different clinical grade camera systems have been used.[87]

A comparative prospective study using sequential imaging showed that both autofluorescence- and ICG-based imaging yielded similar gland detection, efficacy and detection rates (Table 2).[59] The combination of autofluorescence and ICG imaging was also shown to aid visualization of the parathyroid glands and their perfusion via a multi-wavelength fluorescence imaging approach; the glands were localized using autofluorescence, after which administration and subsequent imaging of ICG allowed assessment of the gland's perfusion. Autofluorescence allowed visualization of the glands in 75-87.3% of cases, while the ICG signal in both the gland and its vasculature provided surgical guidance in the remaining cases (Figure 4).[60,62] In a different setting using the same method, combined use of autofluorescence- and ICG-based detection yielded a sensitivity of 82% and 81%, respectively.[61] Slightly in contrast to the above, the latter study indicated autofluorescence provided target delineation, while ICG helped determine the degree of gland vascularization.

Experimental extensions. Dyes such as PpIX and MB have also been assessed for use in parathyroid identification.[87] However, despite their approval for clinical use, the toxicity profiles of these dyes could limit their implementation.[88-90] Especially considering the value provided by the combined use of autofluorescence and ICG imaging. Preclinical efforts in developing new imaging agents for this application yielded 2 additional fluorophores, T700F ($\lambda_{ex\ max}$: 651 nm, $\lambda_{em\ max}$: 665 nm), and T800F ($\lambda_{ex\ max}$: 758 nm, $\lambda_{em\ max}$: 771 nm), with peak emissions
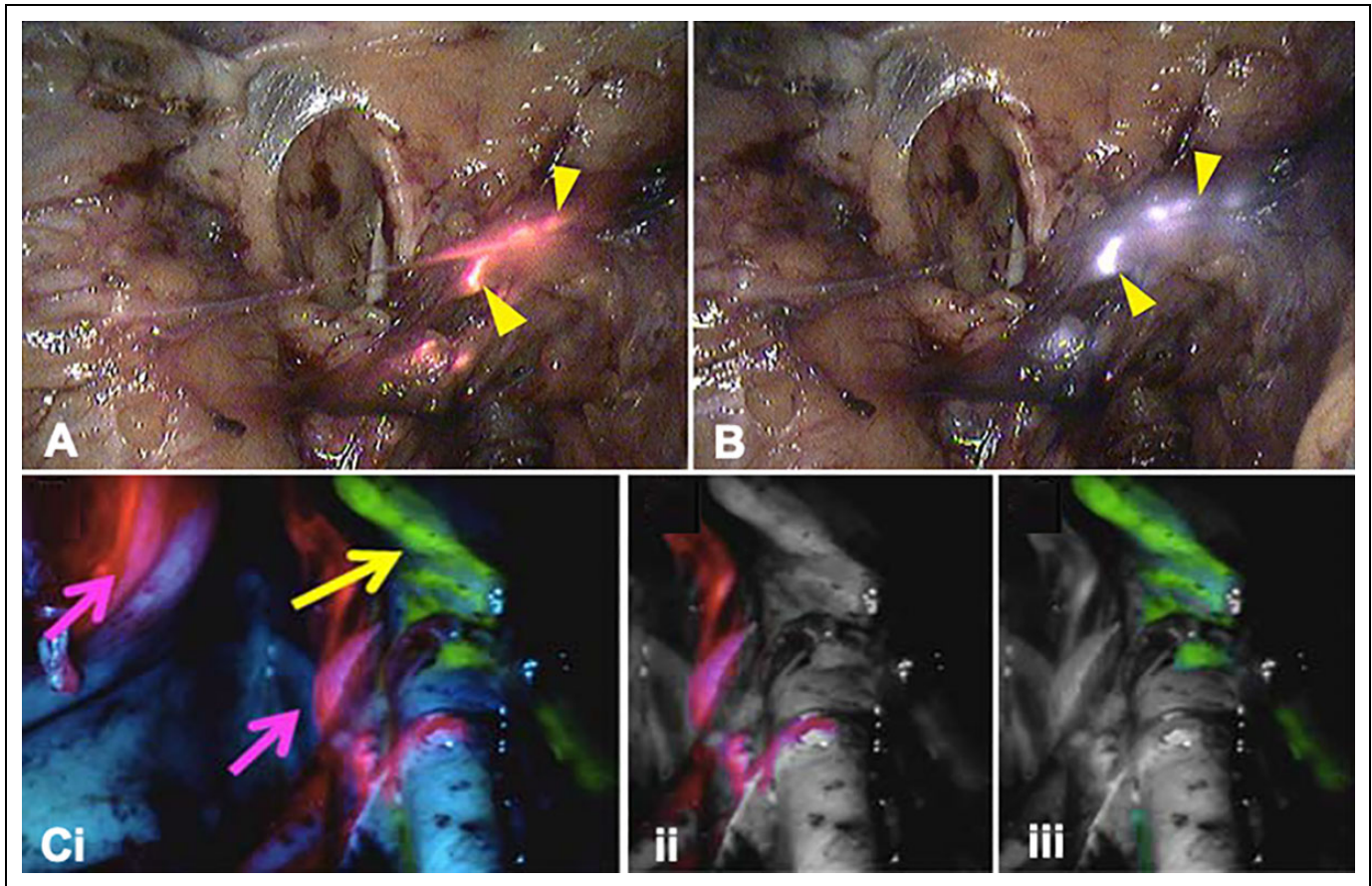
Figure 5. Multi-wavelength imaging of lymph nodes and lymphatic duct. Lymphatic co-localization (yellow arrow heads) of (A) MB and (B) ICG following uterine and cervical injection, respectively, in a patient with endometrial cancer (adapted from Laios et al[63]). (C-i) Unprocessed multi-wavelength image of lymphatic ducts in a porcine model (Fluorescein; yellow arrow) and 2 (ICG-nanocolloid; pink arrow). Digitally separated images of the 2 signals: (ii) ICG and (iii) Fluorescein (adapted from Meershoek et al.[27]).

at 700 nm and 800 nm respectively.[91] In a pig model these dyes allowed real-time distinction of parathyroid and thyroid glands simultaneously in the context of blood and surrounding soft tissue.[91]

Lymphatic Imaging

MB and ICG. Use of ICG is widely adopted for lymphatic imaging applications and over the years has disseminated from Japan to Europe and the US. As blue dyes such as patent blue (visible but not fluorescent) and MB (visible and fluorescent[4]) and the fluorescent dye ICG are often concurrently applied during lymphatic mapping,[92,93] also this indication has benefit from clinical multi-wavelength studies.[20] In addition to the use of the above-mentioned dyes for lymphatic imaging, also the use of Fluorescein has been explored for this indication.[20]

The addition of MB fluorescence to facilitate multi-wavelength fluorescence imaging (Table 2) when combined with ICG has been explored during laparoscopic SN procedures in endometrial cancer (Figure 5A and B) in order to independently examine the aberrant lymphatic drainage.[63] Not only did this study reveal an association between the injection site and

SN location but did also suggest that cervical injection in endometrial cancer might not be fully representative of lymphatic tumor spread. This was highlighted by the fluorescence detection of a paraaortic SN that could only be detected using ICG, after administration in the uterine fundus.[63]

Fluorescein and ICG. In laparoscopic prostate cancer surgery, ICG-based identification of SNs after preoperative administration of ICG-^{99m}Tc-nanocolloid was extended by exploring multi-wavelength fluorescence imaging after intraoperative administration of Fluorescein.[20] The drainage pattern of both dyes differed and helped determine the value of SN specific-(ICG-^{99m}Tc-nanocolloid) versus lymphangiographic tracers (Fluorescein) in robot-assisted surgery. SNs could be discriminated based on the ICG signal, while the Fluorescein signal provided visualization of the corresponding lymph ducts (Table 2).

Experimental extensions. Various preclinical lymphatic imaging efforts have used differently colored fluorescent tracers (mostly nanoparticles) to discriminate between different lymphatic drainage pathways. This concept has been beautifully
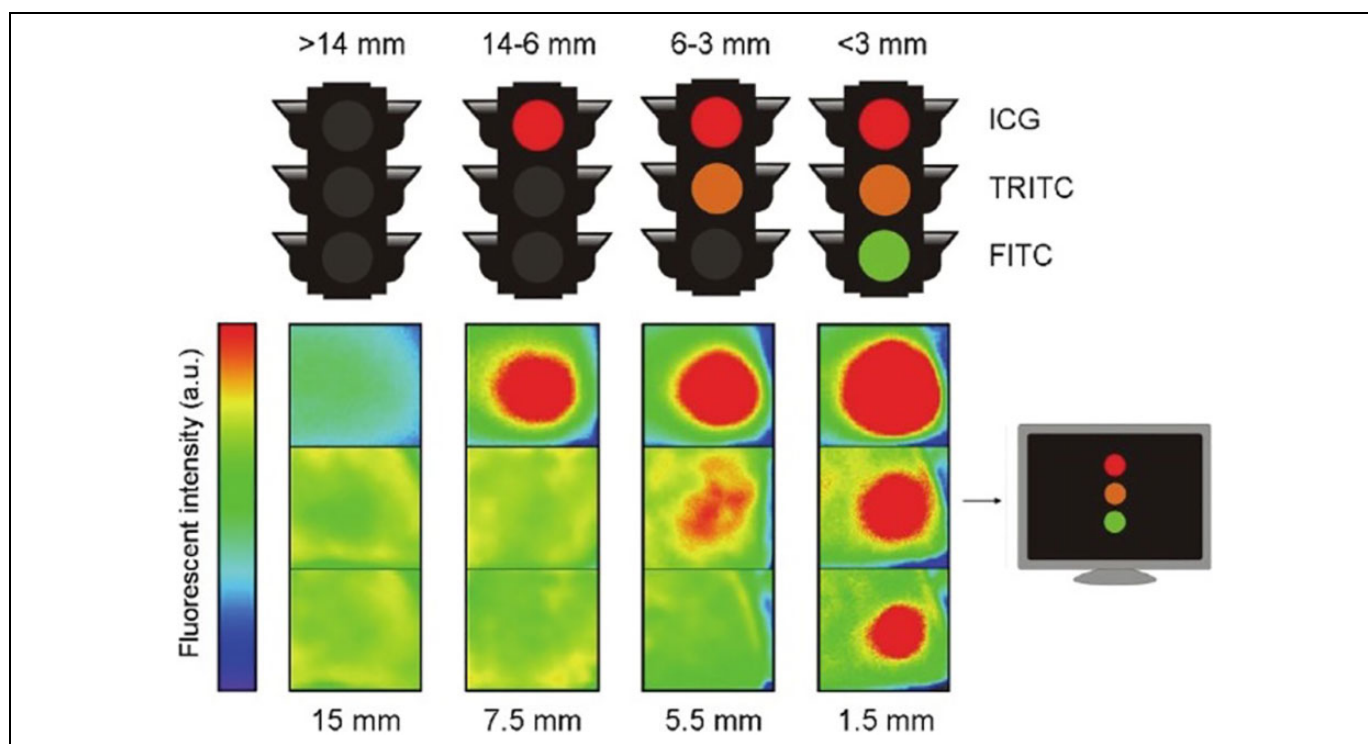
Figure 6. Multiwavelength fluorescence as a means to provide depth assessment. Traffic light analogue for depth estimation using a marker seed filled with a mixture of ICG, TRITC and FITC. Depending on the number of colors used, an estimation of depth can be made based on the tissue penetration of each dye (top illustration). A camera system is required to detect the ICG signal and can aid in visualizing the TRITC and FITC signals (here depicted using (reversed) Rainbow color table; bottom illustration) (Chin et al.[114]).

demonstrated by Kobayashi et al. using quantum dots.[28] Here, the identical excitation properties of quantum dots, combined with their distinct narrow emission spectra, supported the differentiation of 5 different lymphatic drainage patterns in the head and neck area of a mouse.[28] This effort was followed by mouse studies that used fluorescently functionalized immunoglobulins,[94] dendrimers,[95] lipid nanoparticles (lipidots),[96] silicon nanocrystals,[97] bioluminescence resonance energy transfer quantum dot (BRET-Qdot)[98] and lanthanide-based upconversion nanoparticles,[99] or fluorescent core-shell silica nanoparticles conjugated to different melanoma targeting agents.[100]

Clinically, a shift is occurring from "removing nodes that count" to "sparing nodes that are not involved," an approach that could help reduce the incidence of side effects caused by lymphatic dissections in prostate cancer surgery.[101] To address this need, Meershoek et al.[27] assessed the possibility to differentiate between different sections of the lymphatic system using 2 clinically applied tracers: ICG-nanocolloid and Fluorescein (Figure 5C). In a porcine model, Fluorescein was used to visualize the intra-abdominal lymph drainage of the lower limbs, while ICG-nanocolloid allowed identification of prostate-related SNs. Simultaneous multi-wavelength fluorescence imaging of both dyes during robotic surgery executed with a standard Firefly laparoscope (da Vinci Si and Xi, Intuitive Surgical) allowed discrimination between the lymphatic drainage of the limbs and prostate without any overlap in signal.[27] When translated to a clinical setting this approach could

thus be used to simplify the heterogeneity of the complex pelvic anatomy by highlighting the SNs that could possibly harbor metastases (using the ICG signal), while surgically induced damage to healthy lymphatic anatomies can be avoided (based on the Fluorescein signal).

Plastic Surgery

In plastic surgery, the angiographic properties of ICG are used to assess tissue perfusion during flap-reconstruction.[102,103] In a prospective trial Philips et al. used both Fluorescein and ICG to assess the flap necrosis of tissue during reconstructive breast surgery.[64] This study in 32 patients (Table 2) revealed that laser-assisted ICG angiography and Fluorescein angiography both overpredict potential areas of necrosis, although ICG angiography was shown to be more accurate.[64]

Discussion

There are multiple examples in human surgery wherein multiwavelength fluorescence imaging approaches have been evaluated (Table 2). Essentially all current studies are technical feasibility studies in relatively small patient numbers, which means it is currently not possible to assess the impact of multiwavelength fluorescence imaging on clinical care. Hence, we have stayed away from making such assessments. From a technical perspective the studies presented indicate that a select

amount of dyes, allowed for in-human use, have been used to specifically stain structures, their physiological surrounding, or delicate anatomies in close relation to the target lesion (Tables 1 and 2). Here the exception is the use of autofluorescence imaging of endogenous compounds to delineate the target as has been presented in thyroid surgery (Table 2, Figure 4). An alternative non-dye based multi-wavelength imaging method has been presented by the Pogue group, who have used measurements on endogenous hemoglobin and deoxyhemoglobin in breast cancer patients (Table 2).[104-107]

Next to the availability of endogenous and exogenous dyes, a wide range of camera systems, with different excitation sources and emission filters have been successfully implemented in the clinical setting, of which some are manufactured to clinical standards, underscoring that multi-wavelength fluorescence imaging is technically feasible by either sequential or simultaneous imaging (Table 2).

Three trends in multi-wavelength fluorescence imaging approaches become apparent from the clinical examples summarized above (Table 2): 1) The concurrent use of a lesion specific dye (e.g. PpIX[5-ALA, HAL] or CSRP) with an unspecific dye that stains the physiological surrounding of the lesion (Fluorescein or ICG) aid in better visualization of the lesion, 2) The use of different dyes, either targeted or unspecific, to address the heterogeneity of tissue and anatomical structures, or 3) Implementation of multi-wavelength fluorescence imaging in order to stain both the target lesion and the surrounding delicate anatomy that needs to be spared, e.g. a glioma (PpIX[5-ALA]) and the surrounding vasculature (ICG). In the preclinical setting these same approaches have been evaluated in murine and porcine models using a wide variety of dye-functionalized targeting agents. Here it should be repeated that preclinical efforts in the field of multi-wavelength fluorescence imaging are more extensive than the studies listed in the current manuscript. Given the substantial preclinical research efforts in this area and the wealth of receptor-targeted fluorescent agents that are being developed, it is likely that the implementation of multi-wavelength fluorescence guided surgery will be expanded when new agents find their way into the clinic. Although not included in the current overview, it should here be mentioned that "activatable" dyes[108] and nerve specific tracers[109-113] could provide key candidates to extend the number of clinically relevant features that can be studied using multi-wavelength fluorescence imaging. Furthermore, the wavelength dependent tissue penetration of fluorescent dyes may be explored to assess the depth of the target (see Figure 6).[114-116] Next to out-of-the-box extensions in radiological tumor marking,[114,117,118] in the future multi-wavelength fluorescence imaging is likely to impact other surgical indications such as, but not limited to, bone perfusion,[119-121] gastro-intestinal surgery,[122-124] bronchoscopy,[125] breast cancer surgery,[126-128] head and neck surgery,[129-131] ovarian cancer surgery,[132] nerve sparing surgery[110,112,133] and cardiac perfusion and coronary angiography.[134]

Besides the use of conventional fluorescence imaging approaches there are a variety of alternative optical imaging methods available that could potentially enhance surgical guidance by supporting multi-signal imaging solutions. Interestingly, each fluorescent emission is also characterized by its time dependent decay (fluorescence lifetime) which is dependent on the surrounding medium of the dye.[135] Fluorescence lifetime detection as an extra dimension can be used to enhance contrast of fluorescent signals and is being explored in different clinical settings.[136,137] That said there is a plurality of other optical techniques such as narrow band imaging,[138] Raman spectroscopy,[139] optical coherence tomography[140] that may be used, just to name a few that are currently being explored in a clinical setting. Ultimately, these technologies, and others, can be used to further extend the degree of multiplexing during image-guided surgery.

The early clinical implementation of multi-wavelength fluorescence imaging, combined with ongoing experimental efforts and the range of chemical and engineering solutions that can be used to mature this application, indicate that multi-wavelength fluorescence imaging is likely to impact the field of image-guided surgery in the future.

ORCID iDs

Hisataka Kobayashi https://orcid.org/0000-0003-1019-4112
Tessa Buckle https://orcid.org/0000-0003-2980-6895

References

1. van den Berg NS, Miwa M, KleinJan GH, et al. (Near-Infrared) fluorescence-guided surgery under ambient light conditions: a next step to embedment of the technology in clinical routine. *Ann Surg Oncol*. 2016;23(8):2586–2595. doi:10.1245/s10434-016-5186-3

2. Zhang XF, Zhang J, Liu L. Fluorescence properties of twenty fluorescein derivatives: lifetime, quantum yield, absorption and emission spectra. *J Fluoresc*. 2014;24(3):819–826. doi:10.1007/s10895-014-1356-5

3. van Willigen DM, van den Berg NS, Buckle T, et al. Multispectral fluorescence guided surgery; a feasibility study in a phantom using a clinical-grade laparoscopic camera system. *Am J Nucl Med Mol Imaging*. 2017;7(3):138–147.

4. Wada H, Hyun H, Vargas C, et al. Sentinel lymph node mapping of liver. *Ann Surg Oncol*. 2015;22(Suppl 3):S1147–1155. doi:10.1245/s10434-015-4601-5

5. Flynn BP, DSouza AV, Kanick SC, Davis SC, Pogue BW. White light-informed optical properties improve ultrasound-guided

fluorescence tomography of photoactive protoporphyrin IX. *J Biomed Opt*. 2013;18(4):046008. doi:10.1117/1.Jbo.18.4.046008

6. Lozovaya GI, Masinovsky Z, Sivash AA. Protoporphyrin ix as a possible ancient photosensitizer: spectral and photochemical studies. *Orig Life Evol Biosph*. 1990;20:321–330. doi:10.1007/BF01808114

7. Montcel B, Mahieu-Williame L, Armoiry X, Meyronet D, Guyotat J. Two-peaked 5-ALA-induced PpIX fluorescence emission spectrum distinguishes glioblastomas from low grade gliomas and infiltrative component of glioblastomas. *Biomed Opt Express*. 2013;4(4):548–558. doi:10.1364/boe.4.000548

8. Burggraaf J, Kamerling IM, Gordon PB, et al. Detection of colorectal polyps in humans using an intravenously administered fluorescent peptide targeted against c-Met. *Nat Med*. 2015;21(8): 955–961. doi:10.1038/nm.3641

9. Mujumdar RB, Ernst LA, Mujumdar SR, Lewis CJ, Waggoner AS. Cyanine dye labeling reagents: sulfoindocyanine succinimidyl esters. *Bioconjug Chem*. 1993;4(2):105–111.

10. Unkart JT, Chen SL, Wapnir IL, González JE, Harootunian A, Wallace AM. Intraoperative tumor detection using a ratiometric activatable fluorescent peptide: a first-in-human phase 1 study. *Ann Surg Oncol*. 2017;24(11):3167–3173. doi:10.1245/s10434-017-5991-3

11. Klehs K, Spahn C, Endesfelder U, Lee SF, Fürstenberg A, Heilemann M. Increasing the brightness of cyanine fluorophores for single-molecule and superresolution imaging. *Chemphyschem*. 2014;15(4):637–641. doi:10.1002/cphc.201300874

12. de Boer E, Warram JM, Tucker MD, et al. In vivo fluorescence immunohistochemistry: localization of fluorescently labeled cetuximab in squamous cell carcinomas. *Sci Rep*. 2015;5:10169. doi:10.1038/srep10169

13. Mahalingam SM, Kularatne SA, Myers CH, et al. Evaluation of novel tumor-targeted near-infrared probe for fluorescence-guided surgery of cancer. *J Med Chem*. 2018;61(21):9637–9646. doi:10. 1021/acs.jmedchem.8b01115

14. Hoogstins CE, Tummers QR, Gaarenstroom KN, et al. A novel tumor-specific agent for intraoperative near-infrared fluorescence imaging: a translational study in healthy volunteers and patients with ovarian cancer. *Clin Cancer Res*. 2016;22(12):2929–2938. doi:10.1158/1078-0432.Ccr-15-2640

15. *Photoimmunotherapy (PIT) Study in Recurrent Head/Neck Cancer for Patients Who Have Failed at Least Two Lines of Therapy*. 2018 ed. National Library of Medicine (US); 2018. clinicaltrials. gov. Accessed March/April, 2020.

16. Lavis LD, Raines RT. Bright ideas for chemical biology. *ACS Chem Biol*. 2008;3(3):142–155. doi:10.1021/cb700248m

17. *Performance of SGM-101 for the Delineation of Primary and Recurrent Tumor and Metastases in Patients Undergoing Surgery for Colorectal Cancer*. 2018 ed. National Library of Medicine (US); 2018. Clinicaltrial.gov. Accessed March/April, 2020.

18. Gutowski M, Framery B, Boonstra MC, et al. SGM-101: an innovative near-infrared dye-antibody conjugate that targets CEA for fluorescence-guided surgery. *Surg Oncol*. 2017;26(2):153–162. doi:10.1016/j.suronc.2017.03.002

19. *Fluorescence-guided Surgery Using cRGD-ZW800-1 in Oral Cancer 09/12/2019 ed*. National Library of Medicine (US); 2019. Clinicaltrials.gov. Accessed March/April, 2020.

20. van den Berg NS, Buckle T, KleinJan GH, van der Poel HG, van Leeuwen FWB. Multispectral fluorescence imaging during robot-assisted laparoscopic sentinel node biopsy: a first step towards a fluorescence-based anatomic roadmap. *Eur Urol*. 2017;72(1): 110–117. doi:10.1016/j.eururo.2016.06.012

21. Jorzik JJ, Bindewald A, Dithmar S, Holz FG. Digital simultaneous fluorescein and indocyanine green angiography, autofluorescence, and red-free imaging with a solid-state laser-based confocal scanning laser ophthalmoscope. *Retina*. 2005;25(4): 405–416. doi:10.1097/00006982-200506000-00003

22. Hensbergen AW, Buckle T, van Willigen DM, et al. Hybrid tracers based on cyanine backbones targeting prostate-specific membrane antigen: tuning pharmacokinetic properties and exploring dye-protein interaction. *J Nucl Med*. 2020;61(2):234–241. doi:10. 2967/jnumed.119.233064

23. Hachamovitch R. Clinical application of rest thallium-201/Stress technetium-99 m sestamibi dual isotope myocardial perfusion single-photon emission computed tomography. *Cardiol Rev*. 1999;7(2):83–91. doi:10.1097/00045415-199903000-00011

24. Schulz RB, Semmler W. Fundamentals of optical imaging. *Handb Exp Pharmacol*. 2008;(185 pt 1):3–22. doi:10.1007/978-3-540-72718-7_1

25. Levenson RM, Lynch DT, Kobayashi H, Backer JM, Backer MV. Multiplexing with multispectral imaging: from mice to microscopy. *Ilar J*. 2008;49(1):78–88. doi:10.1093/ilar.49.1.78

26. Gobel W, Brucker D, Kienast Y, et al. Optical needle endoscope for safe and precise stereotactically guided biopsy sampling in neurosurgery. *Opt Express*. 2012;20(24):26117–26126. doi:10. 1364/oe.20.026117

27. Meershoek P, KleinJan GH, van Oosterom MN, et al. Multispectral-fluorescence imaging as a tool to separate healthy from disease-related lymphatic anatomy during robot-assisted laparoscopy. *J Nucl Med*. 2018;59(11):1757–1760. doi:10.2967/jnumed.118.211888

28. Kobayashi H, Hama Y, Koyama Y, et al. Simultaneous multicolor imaging of five different lymphatic basins using quantum dots. *Nano Lett*. 2007;7(6):1711–1716. doi:10.1021/nl0707003

29. Dickinson ME, Bearman G, Tille S, Lansford R, Fraser SE. Multispectral imaging and linear unmixing add a whole new dimension to laser scanning fluorescence microscopy. *Biotechniques*. 2001; 31(6):1272, 1274–1276, 1278. doi:10.2144/01316bt01

30. Zimmermann T, Marrison J, Hogg K, O'Toole P. Clearing up the signal: spectral imaging and linear unmixing in fluorescence microscopy. *Methods Mol Biol*. 2014;1075:129–148. doi:10. 1007/978-1-60761-847-8_5

31. Sexton KJ, Zhao Y, Davis SC, Jiang S, Pogue BW. Optimization of fluorescent imaging in the operating room through pulsed acquisition and gating to ambient background cycling. *Biomed Opt Express*. 2017;8(5):2635–2648. doi:10.1364/boe.8.002635

32. van den Bos J, Wieringa FP, Bouvy ND, Stassen LPS. Optimizing the image of fluorescence cholangiography using ICG: a systematic review and ex vivo experiments. *Surg Endosc*. 2018;32(12): 4820–4832. doi:10.1007/s00464-018-6233-x

33. Chin PT, Welling MM, Meskers SC, Olmos RAV, Tanke H, van Leeuwen FWB. Optical imaging as an expansion of nuclear medicine: Cerenkov-based luminescence vs fluorescence-based

luminescence. *Eur J Nucl Med Mol Imaging*. 2013;40(8): 1283–1291. doi:10.1007/s00259-013-2408-9

34. Kosaka N, Ogawa M, Sato N, Choyke PL, Kobayashi H. In vivo real-time, multicolor, quantum dot lymphatic imaging. *J Invest Dermatol*. 2009;129(12):2818–2822. doi:10.1038/jid.2009.161

35. Urano Y, Sakabe M, Kosaka N, et al. Rapid cancer detection by topically spraying a gamma-glutamyltranspeptidase-activated fluorescent probe. *Sci Transl Med*. 2011;3(110):110ra119. doi:10.1126/scitranslmed.3002823

36. Kosaka N, Ogawa M, Choyke PL, Kobayashi H. Clinical implications of near-infrared fluorescence imaging in cancer. *Future Oncol*. 2009;5(9):1501–1511. doi:10.2217/fon.09.109

37. Carr JA, Franke D, Caram JR, et al. Shortwave infrared fluorescence imaging with the clinically approved near-infrared dye indocyanine green. *Proc Natl Acad Sci U S A*. 2018;115(17): 4465–4470. doi:10.1073/pnas.1718917115

38. Vahrmeijer AL, Hutteman M, van der Vorst JR, van de Velde CJH, Frangioni JV. Image-guided cancer surgery using near-infrared fluorescence. *Nat Rev Clin Oncol*. 2013;10(9):507–518. doi:10.1038/nrclinonc.2013.123

39. van Leeuwen FW, Hardwick JC, van Erkel AR. Luminescence-based imaging approaches in the field of interventional molecular imaging. *Radiology*. 2015;276(1):12–29. doi:10.1148/radiol.2015132698

40. Hu Z, Fang C, Li B, et al. First-in-human liver-tumour surgery guided by multispectral fluorescence imaging in the visible and near-infrared-I/II windows. *Nat Biomed Eng*. 2020;4(3):259–271. doi:10.1038/s41551-019-0494-0

41. Deal J, Mayes S, Browning C, et al. Identifying molecular contributors to autofluorescence of neoplastic and normal colon sections using excitation-scanning hyperspectral imaging. *J Biomed Opt*. 2018;24(2):1–11. doi:10.1117/1.Jbo.24.2.021207

42. Rich RM, Mummert M, Gryczynski Z, et al. Elimination of autofluorescence in fluorescence correlation spectroscopy using the AzaDiOxaTriAngulenium (ADOTA) fluorophore in combination with time-correlated single-photon counting (TCSPC). *Anal Bioanal Chem*. 2013;405(14):4887–4894. doi:10.1007/s00216-013-6879-0

43. Kim SW, Lee HS, Lee KD. Intraoperative real-time localization of parathyroid gland with near infrared fluorescence imaging. *Gland Surg*. 2017;6(5):516–524. doi:10.21037/gs.2017.05.08

44. McWade MA, Paras C, White LM, Phay JE, Mahadevan-Jansen A, Broome JT. A novel optical approach to intraoperative detection of parathyroid glands. *Surgery*. 2013;154(6):1371–1377; discussion 1377. doi:10.1016/j.surg.2013.06.046

45. Ewelt C, Nemes A, Senner V, et al. Fluorescence in neurosurgery: its diagnostic and therapeutic use. Review of the literature. *J Photochem Photobiol B*. 2015;148:302–309. doi:10.1016/j.jphotobiol.2015.05.002

46. Maugeri R, Villa A, Pino M, et al. With a little help from my friends: the role of intraoperative fluorescent dyes in the surgical management of high-grade gliomas. *Brain Sci*. 2018;8(2):31. doi:10.3390/brainsci8020031

47. Acerbi F, Restelli F, Broggi M, Schiariti M, Ferroli P. Feasibility of simultaneous sodium fluorescein and indocyanine green injection in neurosurgical procedures. *Clin Neurol Neurosurg*. 2016;146:123–129. doi:10.1016/j.clineuro.2016.05.003

48. Lane B, Bohnstedt BN, Cohen-Gadol AA. A prospective comparative study of microscope-integrated intraoperative fluorescein and indocyanine videoangiography for clip ligation of complex cerebral aneurysms. *J Neurosurg*. 2015;122(3): 618–626. doi:10.3171/2014.10.Jns132766

49. Francaviglia N, Iacopino DG, Costantino G, et al. Fluorescein for resection of high-grade gliomas: a safety study control in a single center and review of the literature. *Surg Neurol Int*. 2017;8:145. doi:10.4103/sni.sni_89_17

50. Della Puppa A, Munari M, Gardiman MP, Volpin F. Combined fluorescence using 5-aminolevulinic acid and fluorescein sodium at glioblastoma border: intraoperative findings and histopathologic data about 3 newly diagnosed consecutive cases. *World Neurosurg*. 2019;122:e856–e863. doi:10.1016/j.wneu.2018.10.163

51. Yano H, Nakayama N, Ohe N, Miwa K, Shinoda J, Iwama T. Pathological analysis of the surgical margins of resected glioblastomas excised using photodynamic visualization with both 5-aminolevulinic acid and fluorescein sodium. *J Neurooncol*. 2017;133(2):389–397. doi:10.1007/s11060-017-2445-5

52. Schwake M, Stummer W, Suero Molina EJ, Wölfer J. Simultaneous fluorescein sodium and 5-ALA in fluorescence-guided glioma surgery. *Acta Neurochir (Wien)*. 2015;157(5):877–879. doi:10.1007/s00701-015-2401-0

53. Suero Molina E, Ewelt C, Warneke N, et al. Dual labeling with 5-aminolevulinic acid and fluorescein in high-grade glioma surgery with a prototype filter system built into a neurosurgical microscope: technical note. *J Neurosurg*. 2019:1–7. doi:10.3171/2018.12.Jns182422

54. Suero Molina E, Stummer W. Where and when to cut? Fluorescein guidance for brain stem and spinal cord tumor surgery-technical note. *Oper Neurosurg (Hagerstown)*. 2018;15(3): 325–331. doi:10.1093/ons/opx269

55. Eyupoglu IY, Hore N, Fan Z, et al. Intraoperative vascular DIVA surgery reveals angiogenic hotspots in tumor zones of malignant gliomas. *Sci Rep*. 2015;5:7958. doi:10.1038/srep07958

56. Marien A, Rock A, Maadarani KE, et al. Urothelial tumors and dual-band imaging: a new concept in confocal laser endomicroscopy. *J Endourol*. 2017;31(5):538–544. doi:10.1089/end.2016.0892

57. Kriegmair MC, Rother J, Grychtol B, et al. Multiparametric cystoscopy for detection of bladder cancer using real-time multispectral imaging. *Eur Urol*. 2020;77(2):251–259. doi:10.1016/j.eururo.2019.08.024

58. Kaibori M, Matsui K, Ishizaki M, et al. Intraoperative detection of superficial liver tumors by fluorescence imaging using indocyanine green and 5-aminolevulinic acid. *Anticancer Res*. 2016; 36(4):1841–1849.

59. Kahramangil B, Berber E. Comparison of indocyanine green fluorescence and parathyroid autofluorescence imaging in the identification of parathyroid glands during thyroidectomy. *Gland Surg*. 2017;6(6):644–648. doi:10.21037/gs.2017.09.04

60. Alesina PF, Meier B, Hinrichs J, Mohmand W, Walz MK. Enhanced visualization of parathyroid glands during video-

assisted neck surgery. *Langenbecks Arch Surg*. 2018;403(3): 395–401. doi:10.1007/s00423-018-1665-2

61. Lerchenberger M, Al Arabi N, Gallwas JKS, Stepp H, Hallfeldt KKJ, Ladurner R. Intraoperative near-infrared autofluorescence and indocyanine green imaging to identify parathyroid glands: a comparison. *Int J Endocrinol*. 2019;2019:4687951. doi:10.1155/2019/4687951

62. Ladurner R, Lerchenberger M, Al Arabi N, Gallwas JKS, Stepp H, Hallfeldt KKJ. Parathyroid autofluorescence—how does it affect parathyroid and thyroid surgery? A 5 year experience. *Molecules (Basel, Switzerland)*. 2019;24(14):2560. doi:10.3390/molecules24142560

63. Laios A, Volpi D, Tullis ID, et al. A prospective pilot study of detection of sentinel lymph nodes in gynaecological cancers using a novel near infrared fluorescence imaging system. *BMC Res Notes*. 2015;8:608. doi:10.1186/s13104-015-1576-z

64. Phillips BT, Lanier ST, Conkling N, et al. Intraoperative perfusion techniques can accurately predict mastectomy skin flap necrosis in breast reconstruction: results of a prospective trial. *Plast Reconstr Surg*. 2012;129(5):778e–788e. doi:10.1097/PRS.0b013e31824a2ae8

65. Zhao X, Belykh E, Cavallo C, et al. Application of fluorescein fluorescence in vascular neurosurgery. *Front Surg*. 2019;6:52. doi:10.3389/fsurg.2019.00052

66. Stummer W, Pichlmeier U, Meinel T, et al. Fluorescence-guided surgery with 5-aminolevulinic acid for resection of malignant glioma: a randomised controlled multicentre phase III trial. *Lancet Oncol*. 2006;7(5):392–401. doi:10.1016/s1470-2045(06)70665-9

67. Hadjipanayis CG, Stummer W, Sheehan JP. 5-ALA fluorescence-guided surgery of CNS tumors. *J Neurooncol*. 2019;141(3): 477–478. doi:10.1007/s11060-019-03109-y

68. Senders JT, Muskens IS, Schnoor R, et al. Agents for fluorescence-guided glioma surgery: a systematic review of preclinical and clinical results. *Acta Neurochir (Wien)*. 2017;159(1): 151–167. doi:10.1007/s00701-016-3028-5

69. O'Brien T, Ray E, Chatterton K, Khan MS, Chandra A, Thomas K. Prospective randomized trial of hexylaminolevulinate photodynamic-assisted transurethral resection of bladder tumour (TURBT) plus single-shot intravesical mitomycin C vs conventional white-light TURBT plus mitomycin C in newly presenting non-muscle-invasive bladder cancer. *BJU Int*. 2013;112(8): 1096–1104. doi:10.1111/bju.12355

70. Burger M, Grossman HB, Droller M, et al. Photodynamic diagnosis of non-muscle-invasive bladder cancer with hexaminolevulinate cystoscopy: a meta-analysis of detection and recurrence based on raw data. *Eur Urol*. 2013;64(5):846–854. doi:10.1016/j.eururo.2013.03.059

71. Mariappan P, Rai B, El-Mokadem I, et al. Real-life experience: early recurrence with Hexvix photodynamic diagnosis-assisted transurethral resection of bladder tumour vs good-quality white light TURBT in new non-muscle-invasive bladder cancer. *Urology*. 2015;86(2):327–331. doi:10.1016/j.urology.2015.04.015

72. Saint F, Elalouf V, Spie R, et al. Prospective monocentric evaluation of bladder tumor targeting by Hexvix(R) fluorescence: preliminary results [in French]. *Prog Urol*. 2010;20(9):644–650. doi:10.1016/j.purol.2010.04.007

73. Villa L, Cloutier J, Cote JF, Salonia A, Montorsi F, Traxer O. Confocal laser endomicroscopy in the management of endoscopically treated upper urinary tract transitional cell carcinoma: preliminary data. *J Endourol*. 2016;30(2):237–242. doi:10.1089/end.2015.0644

74. Pan Y, Volkmer JP, Mach KE, et al. Endoscopic molecular imaging of human bladder cancer using a CD47 antibody. *Sci Transl Med*. 2014;6(260):260ra148. doi:10.1126/scitranslmed.3009457

75. Kiss B, van den Berg NS, Ertsey R, et al. CD47-targeted near-infrared photoimmunotherapy for human bladder cancer. *Clin Cancer Res*. 2019;25(12):3561–3571. doi:10.1158/1078-0432.Ccr-18-3267

76. Ishizawa T, Fukushima N, Shibahara J, et al. Real-time identification of liver cancers by using indocyanine green fluorescent imaging. *Cancer*. 2009;115(11):2491–2504. doi:10.1002/cncr.24291

77. Inoue Y, Tanaka R, Komeda K, Hirokawa F, Hayashi M, Uchiyama K. Fluorescence detection of malignant liver tumors using 5-aminolevulinic acid-mediated photodynamic diagnosis: principles, technique, and clinical experience. *World J Surg*. 2014;38(7):1786–1794. doi:10.1007/s00268-014-2463-9

78. Schneider C, Johnson SP, Gurusamy K, et al. Identification of liver metastases with probe-based confocal laser endomicroscopy at two excitation wavelengths. *Lasers Surg Med*. 2017;49(3): 280–292. doi:10.1002/lsm.22617

79. Nakaseko Y, Ishizawa T, Saiura A. Fluorescence-guided surgery for liver tumors. *J Surg Oncol*. 2018;118(2):324–331. doi:10.1002/jso.25128.

80. Ashitate Y, Stockdale A, Choi HS, Laurence RG, Frangioni JV. Real-time simultaneous near-infrared fluorescence imaging of bile duct and arterial anatomy. *J Surg Res*. 2012;176(1):7–13. doi:10.1016/j.jss.2011.06.027

81. Bhavane R, Starosolski Z, Stupin I, Ghaghada KB, Annapragada A. NIR-II fluorescence imaging using indocyanine green nanoparticles. *Sci Rep*. 2018;8(1):14455. doi:10.1038/s41598-018-32754-y

82. Framery B, Gutowski M, Dumas K, et al. Toxicity and pharmacokinetic profile of SGM-101, a fluorescent anti-CEA chimeric antibody for fluorescence imaging of tumors in patients. *Toxicol Rep*. 2019;6:409–415. doi:10.1016/j.toxrep.2019.04.011

83. Fanaropoulou NM, Chorti A, Markakis M, Papaioannou M, Michalopoulos A, Papavramidis T.The use of indocyanine green in endocrine surgery of the neck: a systematic review. *Medicine (Baltimore)*. 2019;98(10):e14765. doi:10.1097/md.0000000000014765

84. Rudin AV, Berber E. Impact of fluorescence and autofluorescence on surgical strategy in benign and malignant neck endocrine diseases. *Best Pract Res Clin Endocrinol Metab*. 2019; 33(4):101311. doi:10.1016/j.beem.2019.101311

85. Solorzano CC, Thomas G, Baregamian N, Mahadevan-Jansen A. Detecting the near infrared autofluorescence of the human parathyroid: hype or opportunity [published online December 2, 2019]? *Ann Surg*. 2019. doi:10.1097/sla.0000000000003700

86. Spartalis E, Ntokos G, Georgiou K, et al. Intraoperative Indocyanine Green (ICG) angiography for the identification of the

parathyroid glands: current evidence and future perspectives. *In Vivo*. 2020;34(1):23–32. doi:10.21873/invivo.11741

87. Abbaci M, De Leeuw F, Breuskin I, et al. Parathyroid gland management using optical technologies during thyroidectomy or parathyroidectomy: a systematic review. *Oral Oncol*. 2018; 87:186–196.doi:10.1016/j.oraloncology.2018.11.011

88. Ackroyd R, Brown N, Vernon D, et al. 5-Aminolevulinic acid photosensitization of dysplastic Barrett's esophagus: a pharmacokinetic study. *Photochem Photobiol*. 1999;70:656–662.

89. Ginimuge PR, Jyothi SD. Methylene blue: revisited. *J Anaesthesiol Clin Pharmacol*. 2010;26(4):517–520.

90. Herman MA, Webber J, Fromm D, Kessel D. Hemodynamic effects of 5-aminolevulinic acid in humans. *J Photochem Photobiol B*. 1998;43(1):61–65. doi:10.1016/s1011-1344(98)00086-4

91. Hyun H, Park MH, Owens EA, et al. Structure-inherent targeting of near-infrared fluorophores for parathyroid and thyroid gland imaging. *Nat Med*. 2015;21(2):192–197. doi:10.1038/nm.3728

92. Crane LM, Themelis G, Pleijhuis RG, et al. Intraoperative multi-spectral fluorescence imaging for the detection of the sentinel lymph node in cervical cancer: a novel concept. *Mol Imaging Biol*. 2011;13(5):1043–1049. doi:10.1007/s11307-010-0425-7

93. He K, Chi C, Kou D, et al. Comparison between the indocyanine green fluorescence and blue dye methods for sentinel lymph node biopsy using novel fluorescence image-guided resection equipment in different types of hospitals. *Transl Res*. 2016; 178:74–80. doi:10.1016/j.trsl.2016.07.010

94. Hama Y, Koyama Y, Urano Y, Choyke PL, Kobayashi H. Two-color lymphatic mapping using Ig-conjugated near infrared optical probes. *J Invest Dermatol*. 2007;127(10):2351–2356. doi:10.1038/sj.jid.5700892

95. Kobayashi H, Longmire MR, Ogawa M, Choyke PL, Kawamoto S. Multiplexed imaging in cancer diagnosis: applications and future advances. *Lancet Oncol*. 2010;11(6):589–595. doi:10.1016/s1470-2045(10)70009-7

96. Gravier J, Navarro FP, Delmas T, et al. Lipidots: competitive organic alternative to quantum dots for in vivo fluorescence imaging. *J Biomed Opt*. 2011;16(9):096013. doi:10.1117/1.3625405

97. Erogbogbo F, Yong KT, Roy I, Xu G, Prasad PN, Swihart MT. Biocompatible luminescent silicon quantum dots for imaging of cancer cells. *ACS Nano*. 2008;2(5):873–878. doi:10.1021/nn700319z

98. Kosaka N, Mitsunaga M, Bhattacharyya S, Miller SC, Choyke PL, Kobayashi H. Self-illuminating in vivo lymphatic imaging using a bioluminescence resonance energy transfer quantum dot nano-particle. *Contrast Media Mol Imaging*. 2011;6(1):55–59. doi:10.1002/cmmi.395

99. Cheng L, Yang K, Zhang S, Shao M, Lee S, Liu Z. Highly-sensitive multiplexed in vivo imaging using PEGylated upconversion nanoparticles. *Nano Res*. 2010;3:722–732. doi:10.1007/s12274-010-0036-2

100. Chen F, Madajewski B, Ma K, et al. Molecular phenotyping and image-guided surgical treatment of melanoma using spectrally distinct ultrasmall core-shell silica nanoparticles. *Sci Adv*. 2019; 5:eaax5208. doi:10.1126/sciadv.aax5208

101. Briganti A, Chun FK, Salonia A, et al. Complications and other surgical outcomes associated with extended pelvic lymphadenectomy in men with localized prostate cancer. *Eur Urol*. 2006;50(5):1006–1013. doi:10.1016/j.eururo.2006.08.015

102. Alstrup T, Christensen BO, Damsgaard TE. ICG angiography in immediate and delayed autologous breast reconstructions: peroperative evaluation and postoperative outcomes. *J Plast Surg Hand Surg*. 2018;52(5):307–311. doi:10.1080/2000656x.2018.1486320

103. Jakubietz RG, Schmidt K, Bernuth S, Meffert RH, Jakubietz MG. Evaluation of the intraoperative blood flow of pedicled perforator flaps using indocyanine green-fluorescence angiography. *Plast Reconstr Surg Glob Open*. 2019;7(9):e2462. doi:10.1097/gox.0000000000002462

104. Dehghani H, Pogue BW, Poplack SP, Paulsen KD. Multiwave-length three-dimensional near-infrared tomography of the breast: initial simulation, phantom, and clinical results. *Appl Opt*. 2003;42(1):135–145. doi:10.1364/ao.42.000135

105. McBride TO, Pogue BW, Poplack S, et al. Multispectral near-infrared tomography: a case study in compensating for water and lipid content in hemoglobin imaging of the breast. *J Biomed Opt*. 2002;7(1):72–79. doi:10.1117/1.1428290

106. Srinivasan S, Pogue BW, Carpenter C, et al. Developments in quantitative oxygen-saturation imaging of breast tissue in vivo using multispectral near-infrared tomography. *Antioxid Redox Signal*. 2007;9(8):1143–1156. doi:10.1089/ars.2007.1643

107. Wang J, Pogue BW, Jiang S, Paulsen KD. Near-infrared tomography of breast cancer hemoglobin, water, lipid, and scattering using combined frequency domain and cw measurement. *Opt Lett*. 2010;35(1):82–84. doi:10.1364/ol.35.000082

108. Mochida A, Ogata F, Nagaya T, Choyke PL, Kobayashi H.Activatable fluorescent probes in fluorescence-guided surgery: practical considerations. *Bioorg Med Chem*. 2018;26(4):925–930. doi:10.1016/j.bmc.2017.12.002

109. Buckle T, van der Wal S, van Willigen DM, Aalderink G, Klein-Jan GH, van Leeuwen FWB. Fluorescence background quenching as a means to increase signal to background ratio's—a proof of concept during nerve imaging. *Theranostics*. 2020;10(21):9890–9898. doi:10.7150/thno.46806

110. Gibbs-Strauss SL, Nasr KA, Fish KM, et al. Nerve-highlighting fluorescent contrast agents for image-guided surgery. *Mol Imaging*. 2011;10(2):91–101.

111. Hingorani DV, Whitney MA, Friedman B, et al. Nerve-targeted probes for fluorescence-guided intraoperative imaging. *Theranostics*. 2018;8(15):4226–4237. doi:10.7150/thno.23084

112. Hussain T, Mastrodimos MB, Raju SC, et al. Fluorescently labeled peptide increases identification of degenerated facial nerve branches during surgery and improves functional outcome. *PLoS One*. 2015;10(3):e0119600. doi:10.1371/journal.pone.0119600

113. Walsh EM, Cole D, Tipirneni KE, et al. Fluorescence imaging of nerves during surgery. *Ann Surg*. 2019;270(1):69–76.doi:10.1097/sla.0000000000003130

114. Chin PT, Beekman CA, Buckle T, Josephson L, van Leeuwen FW. Multispectral visualization of surgical safety-margins using fluorescent marker seeds. *Am J Nucl Med Mol Imaging*. 2012; 2(2):151–162.

115. Leblond F, Ovanesyan Z, Davis SC, et al. Analytic expression of fluorescence ratio detection correlates with depth in multi-

spectral sub-surface imaging. *Phys Med Biol*. 2011;56(21): 6823–6837. doi:10.1088/0031-9155/56/21/005

116. Miller SJ, Lee CM, Joshi BP, Gaustad A, Seibel EJ, Wang TD. Targeted detection of murine colonic dysplasia in vivo with flexible multispectral scanning fiber endoscopy. *J Biomed Opt*. 2012;17(2):021103. doi:10.1117/1.Jbo.17.2.021103

117. Buckle T, Chin PT, van den Berg NS, et al. Tumor bracketing and safety margin estimation using multimodal marker seeds: a proof of concept. *J Biomed Opt*. 2010;15(5):056021. doi:10. 1117/1.3503955

118. Chin PT, Buckle T, Aguirre de Miguel A, Meskers SCJ, Janssen RAJ, van Leeuwen FWB. Dual-emissive quantum dots for multi-spectral intraoperative fluorescence imaging. *Biomaterials*. 2010; 31(26):6823–6832. doi:10.1016/j.biomaterials.2010.05.030

119. Hyun H, Owens EA, Wada H, et al. Cartilage-specific near-infrared fluorophores for biomedical imaging. *Angew Chem Int Ed Engl*. 2015;54(30):8648–8652. doi:10.1002/anie.201502287

120. Nakayama H, Kawase T, Okuda K, Wolff LF, Yoshie H. In-vivo near-infrared optical imaging of growing osteosarcoma cell lesions xenografted in mice: dual-channel quantitative evaluation of volume and mineralization. *Acta Radiol*. 2011;52(9): 978–988. doi:10.1258/ar.2011.110131

121. Yoshimatsu H, Steinbacher J, Meng S, et al. Feasibility of bone perfusion evaluation in cadavers using indocyanine green fluorescence angiography. *Plast Reconstr Surg Glob Open*. 2017; 5(11):e1570. doi:10.1097/gox.0000000000001570

122. Ashitate Y, Vooght CS, Hutteman M, Oketokoun R, Choi HS, Frangioni JV. Simultaneous assessment of luminal integrity and vascular perfusion of the gastrointestinal tract using dual-channel near-infrared fluorescence. *Mol Imaging*. 2012;11(4):301–308.

123. Bae SM, Bae DJ, Do EJ, et al. Multi-spectral fluorescence imaging of colon dysplasia invivo using a multi-spectral endoscopy system. *Transl Oncol*. 2019;12(2):226–235. doi:10.1016/ j.tranon.2018.10.006

124. Qiu Z, Khondee S, Duan X, et al. Vertical cross-sectional imaging of colonic dysplasia in vivo with multi-spectral dual axes confocal endomicroscopy. *Gastroenterology*. 2014;146(3): 615–617. doi:10.1053/j.gastro.2014.01.016

125. Abdelsattar ZM, Blackmon SH. Using novel technology to augment complex video-assisted thoracoscopic single basilar segmentectomy. *J Thorac Dis*. 2018;10(Suppl 10):S1168–s1178. doi:10.21037/jtd.2018.02.22

126. Kijanka MM, van Brussel AS, van der Wall E, et al. Optical imaging of pre-invasive breast cancer with a combination of VHHs targeting CAIX and HER2 increases contrast and facilitates tumour characterization. *EJNMMI Res*. 2016;6(1): 14. doi:10.1186/s13550-016-0166-y

127. Koyama Y, Barrett T, Hama Y, Ravizzini G, Choyke PL, Kobayashi H. In vivo molecular imaging to diagnose and sub-type tumors through receptor-targeted optically labeled monoclonal antibodies. *Neoplasia*. 2007;9(12):1021–1029. doi:10. 1593/neo.07787

128. Sano K, Mitsunaga M, Nakajima T, Choyke PL, Kobayashi H. In vivo breast cancer characterization imaging using two monoclonal antibodies activatably labeled with near infrared fluorophores. *Breast Cancer Res*. 2012;14(2):R61. doi:10. 1186/bcr3167

129. Meershoek P, van den Berg NS, Brouwer OR, et al. Three-dimensional tumor margin demarcation using the hybrid tracer indocyanine green-(99m)Tc-Nanocolloid: a proof-of-concept study in tongue cancer patients scheduled for sentinel node biopsy. *J Nucl Med*. 2019;60(6):764–769. doi:10.2967/jnumed. 118.220202

130. Thong PS, Olivo M, Kho KW, et al. Laser confocal endomicroscopy as a novel technique for fluorescence diagnostic imaging of the oral cavity. *J Biomed Opt*. 2007;12(1):014007. doi:10. 1117/1.2710193

131. Wang YW, Kang S, Khan A, Bao PQ, Liu JTC. In vivo multi-plexed molecular imaging of esophageal cancer via spectral endoscopy of topically applied SERS nanoparticles. *Biomed Opt Express*. 2015;6(10):3714–3723. doi:10.1364/boe.6.003714

132. Longmire M, Kosaka N, Ogawa M, et al. Multicolor in vivo targeted imaging to guide real-time surgery of HER2-positive micrometastases in a two-tumor coincident model of ovarian cancer. *Cancer Sci*. 2009;100(6):1099–1104. doi:10.1111/j. 1349-7006.2009.01133.x

133. Grivas N, van der Roest RC, de Korne CM, et al. The value of periprostatic fascia thickness and fascia preservation as prognostic factors of erectile function after nerve-sparing robot-assisted radical prostatectomy. *World J Urol*. 2019;37(2): 309–315. doi:10.1007/s00345-018-2387-3

134. Tanaka E, Chen FY, Flaumenhaft R, et al. Real-time assessment of cardiac perfusion, coronary angiography, and acute intravascular thrombi using dual-channel near-infrared fluorescence imaging. *J Thorac Cardiovasc Surg*. 2009;138(1):133–140. doi:10.1016/j.jtcvs.2008.09.082

135. Palo K, Brand L, Eggeling C, Jäger S, Kask P, Gall K. Fluorescence intensity and lifetime distribution analysis: toward higher accuracy in fluorescence fluctuation spectroscopy. *Biophys J*. 2002;83(2):605–618. doi:10.1016/s0006-3495(02)75195-3

136. Hartl BA, Ma HSW, Sridharan S, et al. Label-free fluorescence lifetime spectroscopy detects radiation-induced necrotic changes in live brain in real-time. *Biomed Opt Express*. 2018;9(8): 3559–3580. doi:10.1364/boe.9.003559

137. Sun Y, Periasamy A. Additional correction for energy transfer efficiency calculation in filter-based Forster resonance energy transfer microscopy for more accurate results. *J Biomed Opt*. 2010;15:020513. doi:10.1117/1.3407655

138. Boeriu A, Boeriu C, Drasovean S, et al. Narrow-band imaging with magnifying endoscopy for the evaluation of gastrointestinal lesions. *World J Gastrointest Endosc*. 2015;7(2):110–120. doi: 10.4253/wjge.v7.i2.110

139. Rostron P, Gerber D. Raman spectroscopy, a review. *Int J Eng Tech Res*. 2016;6(1):50–64.

140. Bondu M, Marques MJ, Moselund PM, Lall G, Bradua A, Podoleanua A. Multispectral photoacoustic microscopy and optical coherence tomography using a single supercontinuum source. *Photoacoustics*. 2018;9:21–30. doi:10.1016/j.pacs.2017.11.002